Title
COMPLEX FRAGMENT EMISSION AT 50 MeV/u: COMPOUND NUCLEI FOREVER?

Permalink
https://escholarship.org/uc/item/91k2k0k9

Author
Bowman, D.R.

Publication Date
1986-11-01

Lawrence Berkeley Laboratory
UNIVERSITY OF CALIFORNIA

Submitted to Physics Letters B

COMPLEX FRAGMENT EMISSION AT 50 MeV/u: COMPOUND NUCLEI FOREVER?

D.R. Bowman, R.J. Charity, R.J. McDonald,
M.A. McMahan, G.J. Wozniak, L.G. Moretto,
W.L. Kehoe, S. Bradley, A.C. Mignerey, A. Moroni,
A. Bracco, I. Iori, and M.N. Namboodiri

November 1986

NUCLEAR SCIENCE DIVISION

Prepared for the U.S. Department of Energy under Contract DE-AC03-76SF00098

LBL-22483

Complex Fragment Emission at 50 MeV/u: Compound Nuclei Forever?

by

D.R. Bowman, R.J. Charity, R.J. McDonald, M.A. McMahan, G.J. Wozniak, and L.G. Moretto
Nuclear Science Division, Lawrence Berkeley Laboratory, University of California, Berkeley, California, 94720

and

W.L. Kehoe, S. Bradley[(a)], and A.C. Mignerey
Department of Chemistry, University of Maryland, College Park, Maryland, 20742

and

A. Moroni, A. Bracco, and I. Iori
INFN and Department of Physics, University of Milano, Via Celoria 16 20133 Milano, Italy

and

M.N. Namboodiri
Nuclear Chemistry Division, Lawrence Livermore National Laboratory, Livermore, California, 94550

Abstract:

Fragments with $12 \leq Z \leq 35$ have been detected in the reaction of 50 MeV/u ^{139}La on ^{12}C and are shown to be produced solely by the binary decay of a compound nucleus formed in an incomplete fusion reaction. The source velocity, c.m. velocities, cross-sections, and angular distributions extracted from the inclusive data are entirely consistent with this mechanism. The binary coincidence data confirm this interpretation and can be quantitatively accounted for by the singles data.

[(a)] Present address: Kaman Sciences, 2560 Huntington Ave., Alexandria, VA 22303.

The recent observation of complex fragment emission in intermediate energy nuclear reactions has been interpreted as evidence for the onset of new reaction mechanisms. At low bombarding energies, virtually the only observed decay modes of excited nuclei are light particle emission, and fission for the heavier elements [1]. This simple and allegedly well understood picture seems to change dramatically as the bombarding energy is raised into the intermediate energy region (10-100 MeV/u), where previously unobserved decay products with masses between alpha particles and fission fragments are produced in easily detectable amounts [2]. Thus the mechanism(s) responsible for their production is a problem of current interest to both experimentalists and theoreticians.

Preliminary experiments at various energies and projectile-target combinations produced mass distributions apparently following a power law [3], in general accordance with widely contrasting theoretical predictions such as those based upon cold fragmentation [4], liquid-vapor equilibrium [5], and the thermal fragmentation of a participant region [6-8].

All of the mechanisms mentioned above have predicted thresholds somewhere above 10 MeV/u bombarding energy. However, in agreement with an earlier theory [9], complex fragment emission from a compound nucleus has been observed at very small incident energies, below 50 MeV total center-of-mass energy, albeit with very low (sub microbarn) cross-sections [10-12]. Furthermore, in a series of experiments starting at this low energy and continuing to 30 MeV/u, it has been verified that the decay of an equilibrated compound nucleus can account for the major production of complex fragments in a process akin to fission [13]. The measured excitation functions with their rapid rise near the barrier and their subsequent flattening at higher energies, together with thermalized kinetic energy spectra and 90° symmetric angular distributions, are quantitatively consistent with compound nucleus decay.

Searching for the elusive new mechanisms at still greater energies, Trockel et al. [14] have performed experiments with ^{12}C, ^{18}O and ^{20}Ne beams on Ag and Au targets at 48 and 84 MeV/u. They have studied fragments of $Z \leq 10$ between 40° and 120° in the lab, and while they conclude that the proposed liquid-gas equilibrium is inconsistent with the observed properties of these fragments, the production mechanism is left as an open question.

Compound nucleus production of complex fragments can be easily distinguished from the other mechanisms mentioned above because the former is a binary process while the latter are multifragmentation processes. In order to establish which type of processes are involved in complex fragment formation we have used the reverse kinematic technique to study a system very similar to that of Trockel et al., namely 50 MeV/u ^{139}La + ^{12}C.

The use of reverse kinematics (projectile much heavier than target) presents many advantages in this kind of experiment. The use of light target nuclei limits the range of impact parameters available and hence the number of sources. The kinematic focusing allows for coverage of a very large angular range in the center-of-mass with a small laboratory acceptance angle, thus enhancing greatly the detection efficiency for both singles and coincidences. Furthermore, the large velocity of the center-of-mass allows one to detect and identify the atomic number of the entire range of products. It is important to have access to products with masses between that of the projectile and the target because in this region a much cleaner differentiation of the mass distributions associated with the different mechanisms is expected. In this letter we will demonstrate that at 50 MeV/u beam energy the fragments intermediate in mass between the target and projectile are produced by the statistical decay of a well characterized hot compound nucleus formed in an incomplete fusion reaction.

Beams of ^{139}La of approximately 10^7 particles/pulse from the Lawrence Berkeley Laboratory Bevalac impinged upon a ^{12}C target of 2.2 mg/cm^2 thickness. The reaction products were observed with two x-y position-sensitive ΔE(gas)-E(Si) telescopes [15], positioned symmetrically about the beam at 5.5°. Each detector subtended an opening angle of 5° in the laboratory, which as mentioned above, corresponded to a very large angular coverage in the center-of-mass (e.g. about 30-85° and 100-165° for near symmetric compound nucleus decay).

Figure 1(a) shows the product invariant cross-sections in the velocity - Z plane for the La + C reaction [16]. The dashed line is an experimental threshold delimiting the events that stop in the Si detector from those that punch-through. A natural division arises at approximately $Z = 12$. Above this value one observes two ridges that meet and merge at about a velocity $V = 0.95\ V_{beam}$ and $Z =$ 35, and continue to $Z \sim 55$, peaking at $Z \sim 48$. Below $Z = 12$, at the base of the lower velocity ridge, is a region of much higher yield peaking at about $0.7\ V_{beam}$.

The fragments above $Z = 12$ are those which we interpret as being produced only in the binary decay of a compound system. The two peaks for each Z in this region correspond to emission forward and backward in the center-of-mass. The peaks are separated by the Coulomb energy the fragments receive during the decay process. The enhancement of events along the two Coulomb ridges is strong evidence for the binary, damped nature of this process. The events with the largest Z values appear to be evaporation residues of compound nuclei formed in incomplete fusion processes, moving with a velocity intermediate between that of the projectile and that for complete fusion. Although the experimental threshold precludes the quantitative analysis of events with fragment atomic numbers between 12 and 20, there is no observable qualitative difference between these events and those with $20 \leq Z \leq 35$.

A second region, below $Z = 12$ and $V \leq 0.9\ V_{beam}$ contains a component with a compound nucleus origin, which is the continuation of the ridge observed above $Z = 12$, along with noncompound components, which correspond to the high-velocity projectile-like fragments observed in ordinary kinematic reactions. One possible source of these fragments may be the target remnant, another could be a small transfer of mass from the projectile to the target similar to the quasi-elastic or deep-inelastic processes seen at lower energy. The detailed origin of these components, which are also present at lower bombarding energies, is not clear and requires additional experimental attention.

An inspection of the same diagrams at lower bombarding energies (figure 1(b,c)) shows a similar pattern of Coulomb ridges characteristic of binary decay. The continuity of these processes as a function of bombarding energy is exhibited by the fact that figure 1(a) is virtually identical to figure 1(b,c). Extensive analysis of the data at these lower energies has proven that fragments with $Z \geq 12$ arise from the binary decay of a compound nucleus formed either in a complete or incomplete fusion process [13,17].

A vivid way of portraying the binary nature of the decay is to plot, for a given Z, the invariant cross-section in the $v_{||}$, $v_{\perp}$ plane, as in figure 2(a). Shown here is a schematic representation of the equilibrium emission of complex fragments from a source formed by fusion of the projectile with approximately one half of the target. The fast moving equilibrated source has a velocity represented by the arrow labelled Vs. This source decays statistically, the main channels being evaporation of neutrons, protons, and alpha particles. The less probable emission of complex fragments appears as a Coulomb circle centered at the arrowhead. Of course each observed fragment will have a partner located on another circle with a radius dependent upon the mass asymmetry of the fragments. Following the binary decay, each of the hot primary fragments evaporates light particles statistically, thus smearing out the Coulomb circles. The dashed lines in the figure correspond to the limits of detector acceptance at 3.0° and 8.0° in the laboratory. The solid area between the lines is the predicted experimental distribution.

In figure 2(b,c,d) the experimental data are presented in the same way as in fig. 2(a) for Z bins of 21-23, 24-26, and 27-29, respectively. The observed distributions exhibit fairly sharp rings, strikingly similar to the schematic representation. Arrows 1, and 3 represent the beam velocity, and the velocity resulting from complete fusion, respectively. Approximately midway in between, the experimentally determined source velocity is indicated by arrow 2. One should note that the circles associated with the various Z bins are centered at approximately the same value of $v_{||}$, suggesting that all of these fragments are emitted from a single source, and that the radii of the circles decrease with increasing Z, as one would expect from Coulombic acceleration of the fragments in the binary decay. This is exactly the behavior expected from the formation and decay of an equilibrated compound nucleus moving with a well-defined velocity.

If the fragments were emitted from a number of sources with a variety of velocities, one would expect an elliptical distribution in velocity space. The observation of circles or very nearly circles, indicates a well-defined source velocity. This implies that reactions leading to the emission of these heavy fragments select a small range of mass transfers and impact parameters. A simple geometric model [18] where only the occluded part of the lighter partner fuses with the heavy partner can offer a qualitative explanation. In this model the cross-section for the fusion product increases linearly with increasing impact parameter, while the probability for complex fragment emission first increases with impact parameter due to the increasing angular momentum, and subsequently decreases because of the sharp decrease in mass and excitation energy deposition. The combination of these factors leads to a rather sharply peaked distribution in impact parameter and hence in velocity [19].

In figure 3 (a) the source velocity extracted from the mean velocities of the forward and backward-emitted fragments is plotted as a function of fragment Z. The source velocities appear constant over the Z range studied, and are intermediate between the beam velocity and the velocity for complete fusion of the projectile and target. The solid line represents the mean source velocity, corresponding to a incompletely fused system incorporating about one-half of the target mass. From the source velocity we infer the mass transfer from momentum conservation, and assuming that mass and energy are transferred proportionally we obtain a source of Z=60, A=146 and containing 284 ± 82 MeV of excitation energy. After transformation to ordinary kinematics, one obtains a value of 53 ± 14 % for the momentum transfer, in agreement with Viola's systematics [20].

From the radii of the circles in velocity space, one can extract the center-of-mass velocities for each Z value and compare them to a calculation of the expected Coulomb velocity assuming two spheres separated by $R = 1.225\ (A_1^{1/3} + A_2^{1/3}) + 2$ fm, as shown in figure 3(b). While differing marginally in absolute magnitude, the extracted velocities follow the Coulomb trend very well, again illustrating the complete relaxation of the fragment kinetic energy required by compound nucleus decay.

The product angular distributions have been integrated over both the forward and backward hemispheres for each Z value in the range of 22-35. The resulting yields are consistent with the $1/\sin\theta$ distribution characteristic of compound nucleus decay at high angular momentum.

Figure 3(c) shows the absolute cross-sections as a function of fragment Z. Within experimental uncertainty the distribution appears to be flat. The power law dependence of the cross-sections predicted by the liquid-vapor and cold fragmentation theories is not apparent. We have compared our data to statistical model calculations using approximate rotating finite range barriers [21]. The calculations for the upper and lower excitation energy bounds (solid lines) reproduce the data to within a factor of two. The fact that this calculation can reproduce the absolute cross-sections to better than one order of magnitude at excitation energies as large as 284 MeV is strong evidence for the statistical nature of the process. Thus the singles data provide robust evidence for compound nucleus decay.

Figure 4(a) presents coincidence data collected in the two telescopes, as a Z_2 versus Z_1 plot. For coincidence events the atomic numbers of the primary fragments should sum to an average of $Z = 60$ (one-half target plus projectile). Corrections for subsequent evaporation from the primary fragments have been done with the evaporation code PACE [22]. The hatched region shows the band where the binary decay events are predicted to lie, and most of the events do indeed lie inside this region. For all mass asymmetries the fragment charges sum to a constant value $Z_1 + Z_2 \sim 55$, the sharpness of which is shown by the projection in figure 4(b). This constant sum virtually excludes any multifragmentation coincidence events. In figure 3(d) a Monte Carlo simulation of binary decay and sequential evaporation incorporating the detector geometry, beam spot size, and beam divergence is compared with the experimental coincidence/singles ratio. The simulation reproduces the data to within 5 % in the Z range of 21-35. This demonstrates that the observed coincidences account for all of the events observed in singles.

We have presented singles data of source velocities, center-of-mass velocities, cross-sections, and parallel versus perpendicular velocity maps for a range of fragment atomic numbers. Also shown were coincident data which showed no evidence of multifragmentation, and could be completely explained with a Monte Carlo simulation of binary decay. All of the evidence is consistent with the picture, proven at lower energies, of a highly excited source resulting from the incomplete fusion of the target and projectile which relaxes and decays as a compound nucleus.

The quest for the mechanism of production of complex fragments has led us to the incontrovertible and surprising conclusion that binary compound nucleus decay still prevails at these very high energies and that no other process is involved in the production of fragments with $Z \geq 12$, other than that of sequential light particle emission for the largest Z values. The large asymmetry in the entrance channel, chosen to sharpen the velocity of the source, leaves the open question of what might happen for more symmetric systems. While we can venture the guess that peripheral collisions would lead to processes similar to those observed for very asymmetric systems, central collisions are still virgin ground in need of exploration.

This work was supported by the Director, Office of Energy Research, Division of Nuclear Physics of the Office of High Energy and Nuclear Physics of the U.S. Department of Energy under Contract DE-AC03-76SF00098.

References

1. R. Vandenbosch and J.R. Huizenga, Nuclear Fission, (Academic Press, New York, 1973).
2. D.J. Fields et al., Phys. Rev. C30 (1984) 1912, and references therein.
3. C.B. Chitwood et al., Phys. Lett. 131B (1983) 291.
4. J. Aichelin, J. Hufner, and R. Ibarra, Phys. Rev. C30 (1984) 107.
5. A.D. Panagiotou, M.W. Curtin, and D.K. Scott, Phys. Rev. C31 (1985) 55.
6. J.P. Bondorf et al., Nucl. Phys. A443 (1985) 321.
7. J.P. Bondorf et al., Nucl. Phys. A444 (1985) 476.
8. H.W. Barz et al., Nucl. Phys. A448 (1986) 753.
9. L.G. Moretto, Nucl. Phys. A247 (1975) 211.
10. L.G. Sobotka et al., Phys. Rev. Lett. 51, (1983) 2187.
11. L.G. Sobotka et al., Phys. Rev. Lett. 53, (1984) 2004.
12. M.A. McMahan et al., Phys. Rev. Lett. 54, (1985) 1995.
13. R.J. Charity et al., Phys. Rev. Lett. 56, (1986) 1354.
14. R. Trockel et al., Gesellschaft fur Schwerionenforschung preprint GSI-85-45 (1985).
15. R.J. McDonald et al, to be published.
16. The velocity has been obtained from the measured energy and charge by use of the empirical mass parameterization $A = 2.17Z + 0.0027Z^2$, which we have found adequate for systems that have undergone extensive evaporation.
17. R.J. Charity et al., Lawrence Berkeley Laboratory preprint LBL-22448 (1986).
18. J.D. Bowman, W.J. Swiatecki and C.F. Tsang, Lawrence Berkeley Laboratory report LBL-2908 (1973), unpublished.
19. R.J. Charity et al., Lawrence Berkeley Laboratory preprint LBL-22447 (1986).
20. V.E. Viola, Jr. et al., Phys Rev. C26 (1982) 178.
21. A.J. Sierk, Phys. Rev. C33 (1986) 2039.
22. A. Gavron, Phys. Rev. C21 (1980) 230.

Figure Captions

Fig. 1 (a) Singles distribution of reaction products plotted as linear contours of invariant cross-section ($(1/V^2)(\partial^2\sigma/\partial\Omega\partial V)$) in the velocity-Z plane for the 50 MeV/u ^{139}La + ^{12}C reaction. The dashed line is the experimental threshold for particles which punch-through the telescope. (b,c) Similar distributions for 30, and 18 MeV/u Nb + Be.

Fig. 2 (a) Schematic representation of the invariant cross section in the $v_{\parallel}$, $v_{\perp}$ plane for complex fragment emission from a compound nucleus with a well-defined velocity, Vs. The Coulomb ring is the locus of events smeared out by sequential evaporation. The geometric limits of the detector are shown by the dashed lines, and the solid area in between is the predicted experimental distribution. (b,c,d) Experimental distributions for various Z bins. Arrows 1,2, and 3 denote the beam velocity, extracted source velocity, and the velocity for complete fusion, respectively.

Fig. 3 (a) Extracted source velocities in terms of the initial beam velocity. The mean source velocity is given by the solid line (~ 0.96 V_{beam}). The velocity for complete fusion is shown by the dashed line. (b) Extracted c.m. velocities compared to a Coulomb calculation assuming a radius of $R = 1.225\,(A_1^{1/3} + A_2^{1/3}) + 2$ fm at emission. The calculation corrects for the sequential evaporation from the primary fragments. (c) Angle-integrated cross-sections compared to a statistical model calculation based on an approximation for rotating finite range barriers, and using the extracted E* = 284 MeV. (d) The experimental coincidence/singles ratio compared to a Monte Carlo simulation (see text).

Fig 4 Scatter plot of the coincidence events between the two telescopes, Z_2 vs. Z_1. The hatched area is the predicted locus of events after correcting for sequential evaporation from the primary fragments. The distribution of the sum of the charges ($Z_1 + Z_2$) is shown in the inset.

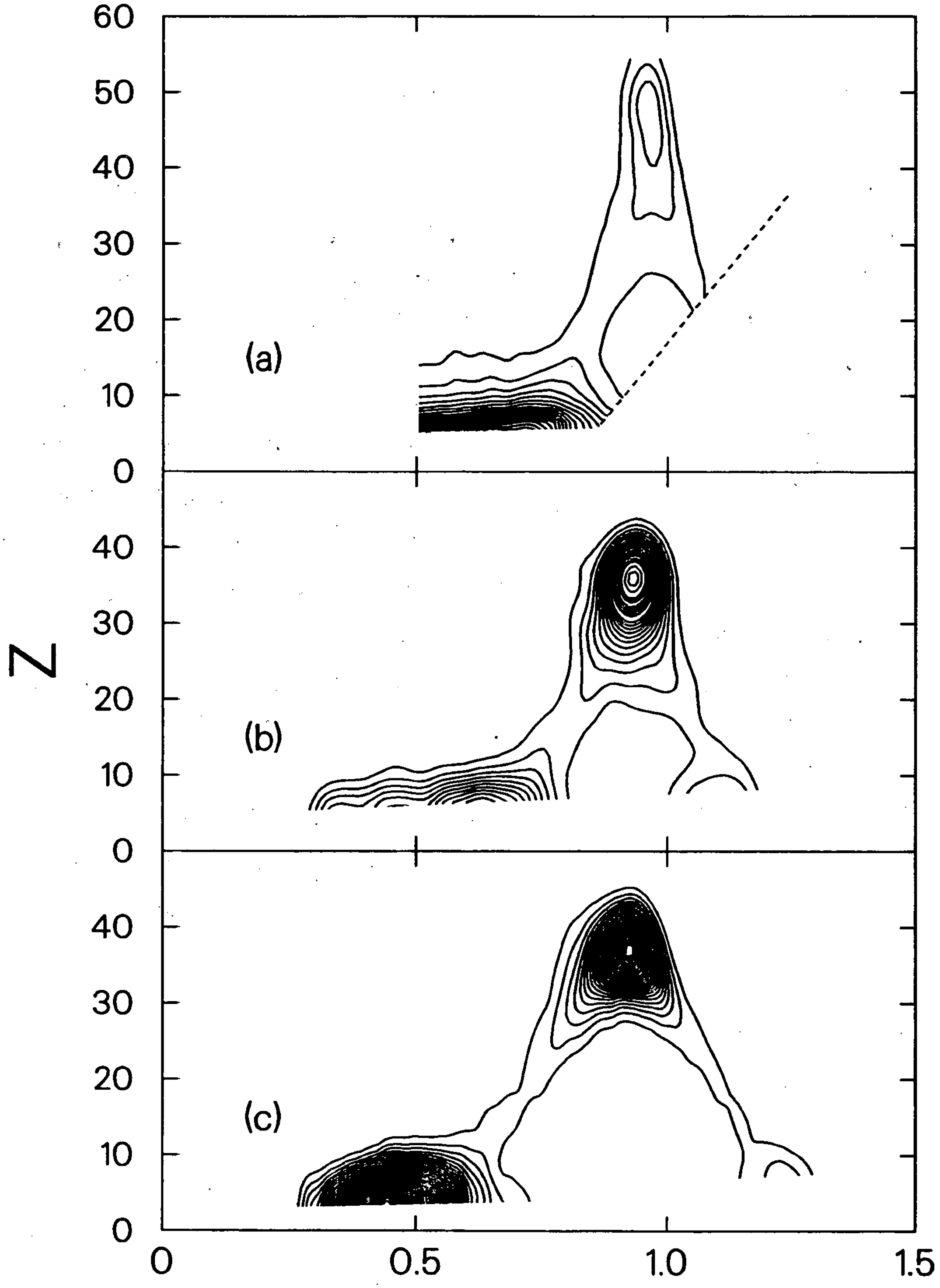

XBL 8611-4289

Fig. 1

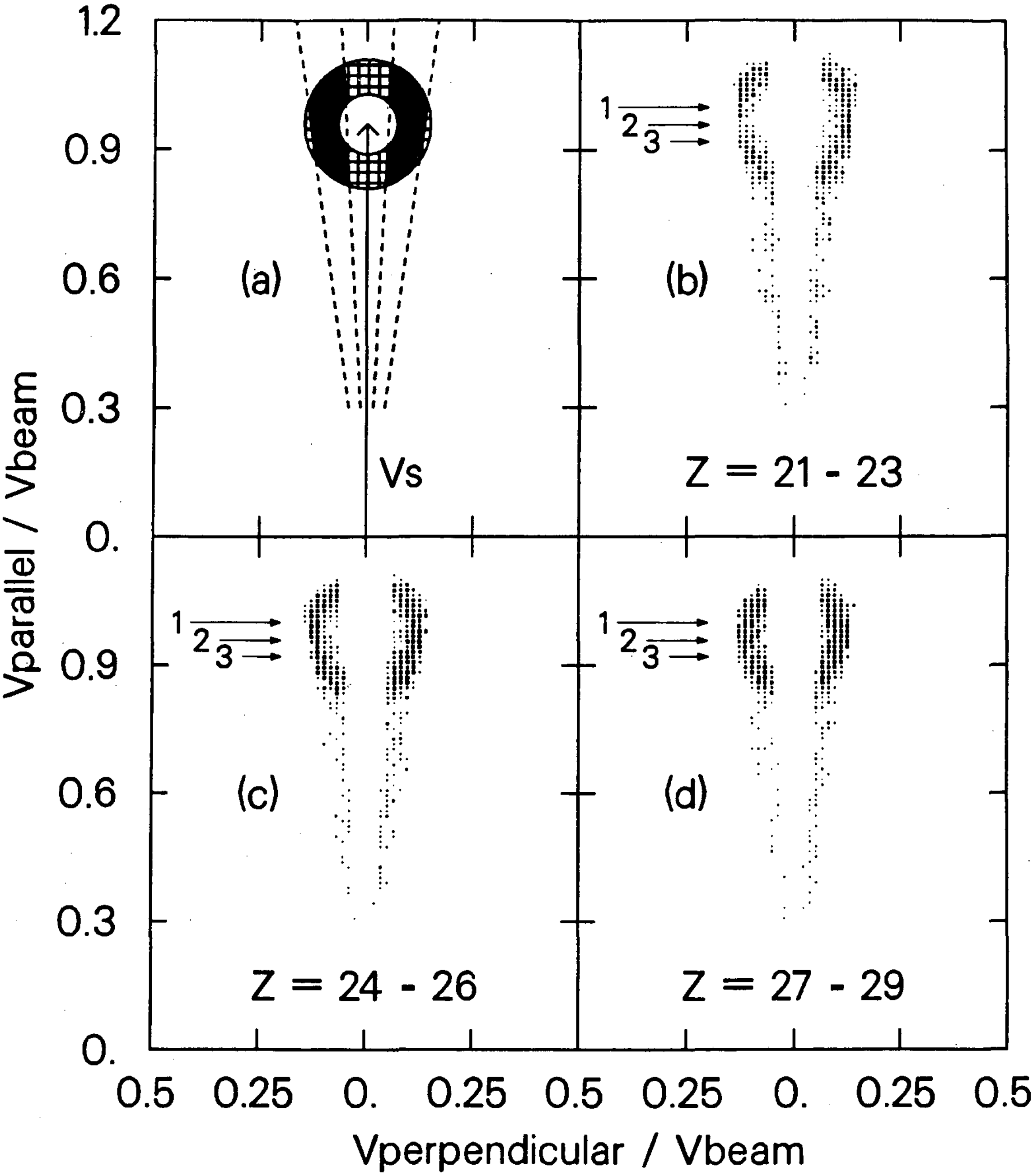

XBL 8611-4288

Fig. 2

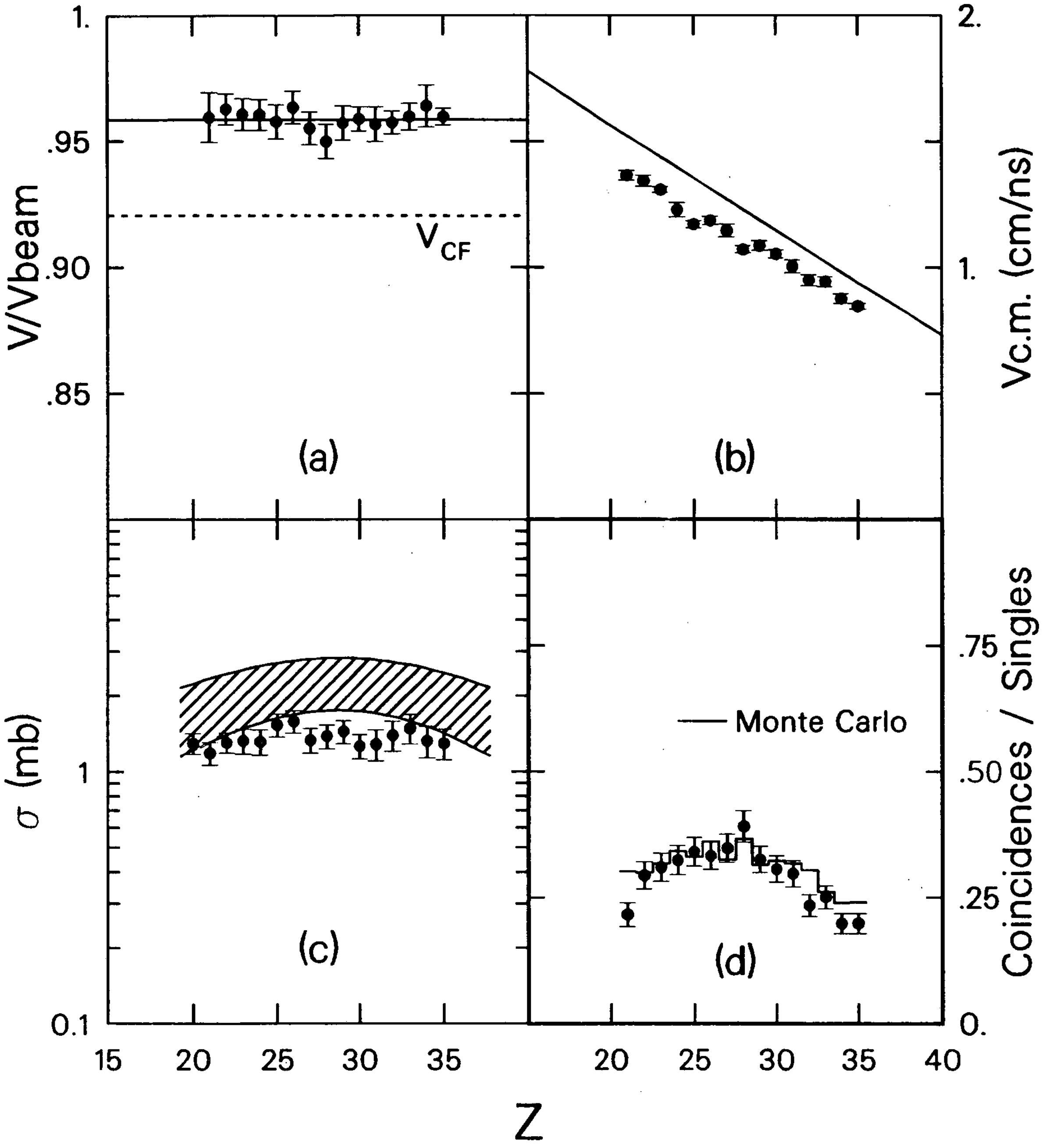

XBL 8611-4287

Fig. 3

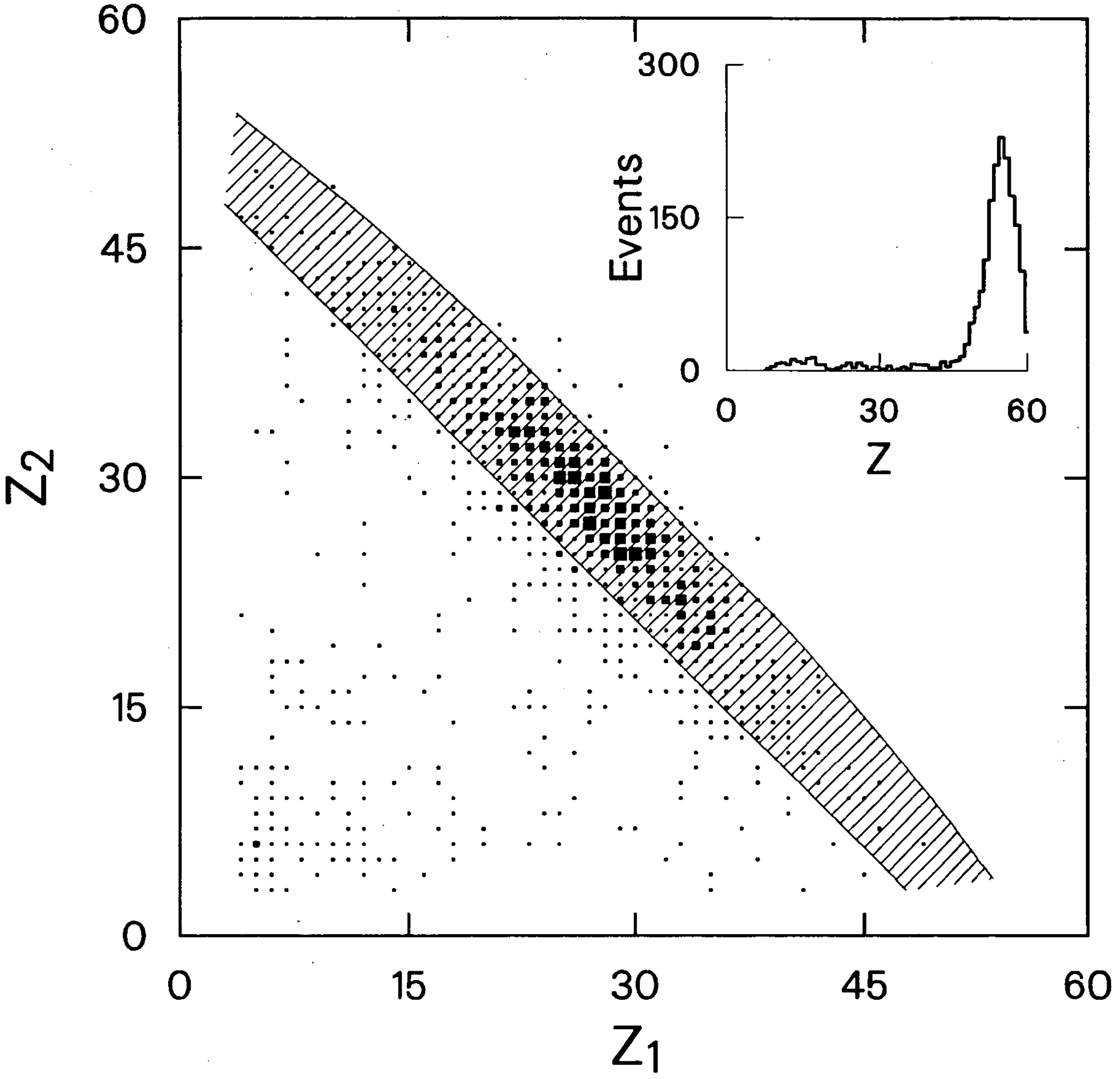
60
45
30
15
0
0
15
30
45
60
Z_2
Z_1
300
150
0
Events
0
30
60
Z

XBL 8611-4286

Fig. 4

LAWRENCE BERKELEY LABORATORY
TECHNICAL INFORMATION DEPARTMENT
UNIVERSITY OF CALIFORNIA
BERKELEY, CALIFORNIA 94720